

Reprinted from the *Soil Science Society of America Journal*
Volume 50, no. 6, November-December 1986
677 South Segoe Rd., Madison, WI 53711 USA

Measurement of Force vs. Time Relations for Waterdrop Impact

M. A. NEARING, J. M. BRADFORD, AND R. D. HOLTZ

Measurement of Force vs. Time Relations for Waterdrop Impact¹

M. A. NEARING, J. M. BRADFORD, AND R. D. HOLTZ²

ABSTRACT

Force vs. time relationships of waterdrop impact are important for understanding the process of erosion caused by soil splash. Waterdrop impact forces were measured for 3.31-, 3.83-, 4.51-, and 5.25-mm diam drops falling from a height of 14.0 m onto piezoelectric transducers with rise times of 2 and 5 μ s. Peak forces occurred within 13 to 21 μ s of initial contact, ranged from 1.0 to 3.8 N, and decreased to 0.5 N after approximately 100 μ s. Average pressures under impact were calculated from the force measurements and an approximation of waterdrop contact area as a function of time and decreased to 100 kPa after 50 μ s. The results indicated that the times and magnitudes of the force of impact were poorly predicted from currently used models and that the compressional wave generated in the water upon impact is probably an important parameter in determining the level and time distribution of forces during impact.

Additional Index Words: erosion, erosivity, raindrop, splash.

Nearing, M.A., J.M. Bradford, and R.D. Holtz. 1986. Measurement of force vs. time relations for waterdrop impact. *Soil Sci. Soc. Am. J.* 50:1532-1536.

MEASUREMENTS OF WATERDROP IMPACT FORCES are needed in order to better understand the mechanics of soil splash by raindrop impact. Recent studies of soil splash have established a relationship between soil shear strength measurements and soil splash detachment (Cruse and Larson, 1977; Al-Durrah and Bradford, 1982a, 1982b; Nearing and Bradford, 1985). Mechanical behavior of soils, and shear strength in particular, is a function of stress, or force per unit area, on a soil mass. The knowledge of waterdrop impact forces (and force-time relationships in particular) is incomplete and must be increased in order to improve the mechanistic description of erosion caused by soil splash.

If numerical methods, such as that used by Huang et al. (1982) to calculate impact pressures on a rigid surface, are to be extended to the more complex situation of computing impact pressures on a nonrigid soil surface, the results of the rigid case must be verified experimentally. Furthermore, measurements of pressure or force of impact on a rigid surface may approximate actual conditions in the case where drop impact causes limited deformation of the soil surface. Such may be the case for soil surface crusts. Therefore, the objective of this study was to measure the force of impact of waterdrops falling at terminal velocity on a rigid surface using piezoelectric transducers. The results will be used to give an approximate quantitative description of impact forces on a soil surface under the conditions approaching that of a rigid surface (such as a soil crust) and to evaluate the numerical tech-

nique of Huang et al. (1982) for computing stresses under waterdrop impact. In particular, the justification of ignoring the propagation of compressional waves in the water during drop impact will be investigated.

BACKGROUND

Attempts have been made to measure waterdrop impact forces. Palmer (1965), using a strain gage, measured the relative stresses of impact of three drop sizes on layers of water ranging from 0 to 30 mm in depth. It is not clear from Palmer's discussion over what area the stress was measured; his values apparently represent a measure of peak force of impact. At zero depth of water the stress caused by impact increased linearly with drop mass for the three drop sizes falling from a height of 1.5 m.

Imeson et al. (1981) obtained measurements of peak voltage of output on a 5-cm diam, 1-mm thick piezoelectric crystal. A direct measure of the true force was not achieved with the crystal. Impact force, F , was estimated from the relation

$$F = m v^2 / 2r \quad [1]$$

where v is impact velocity, m is drop mass, and r is spherical (equivalent) drop radius. The voltage output of the crystal was linearly related ($r^2 = 0.985$) to the assumed impact force as calculated from Eq. [1] and known values of m , v , and r . Equation [1] is derived from classical mechanics and involves several simplifying assumptions of the impact phenomena. Its limitations will be discussed in detail later. The piezoelectric device used by Imeson et al. (1981) acted essentially as an undamped oscillator with an unfiltered output signal. As such, it was useful for measuring peak output voltages which could then be correlated to known or (in the case of force) assumed drop parameters, but the measurements gave no insight into the force-time relationships of impact.

The change in momentum, Δp , of a drop impacting a rigid surface can be expressed as

$$\Delta p = \int_{t_0}^{t_f} F(t) dt = \bar{F} \Delta t \quad [2]$$

where $F(t)$ is the time dependent force of impact, \bar{F} is the average impact force, and Δt is the impact duration from t_0 to t_f . If change in momentum is assumed to be m times v and total impact time is assumed to be $2r/v$, Eq. [1] can be derived from Eq. [2] where \bar{F} from Eq. [1] is \bar{F} , the average force of impact. The assumption (used implicitly by Imeson et al., 1981, to derive Eq. [1]) that the impact time is equal to $2r/v$ implies that the drop is spherical and not oscillating immediately before impact and that the velocity of a fluid particle in the impinging drop does not change prior to reaching the solid surface. Actually, such velocity changes are generated by the propagation of compressional waves in the drop during impact, by surface tension effects, and by fluid viscous effects.

By using the assumptions of no effects due to compressional wave generation or viscous or surface tension, a theoretical force vs. time curve of drop impact may be derived. The force at any given time, as pointed out by Ghadiri and Payne (1977), would be equal to the product of the mass of water arriving at the surface per unit time and its velocity. The area of contact, $A(t)$, of a fluid drop impacting a rigid surface would be a function of the drop shape and velocity.

¹Contribution from the USDA-ARS National Soil Erosion Research Laboratory in cooperation with the Purdue Agric. Exp. Stn. Journal no. 10609. Received 27 Jan. 1986.

²Agricultural Engineer and Soil Scientist, USDA-ARS National Soil Erosion Research Laboratory; and Prof., Dep. of Civil Engineering, Purdue Univ., West Lafayette, IN 47907.

The equilibrium (nonoscillating) shape of the falling drop is oblate (Pruppacher and Pitter, 1971) and described by

$$a = r \left[1 + \sum_{n=0}^{\infty} c_n \cos(n\theta) \right] \quad [3]$$

where a is the radius from the drop center to the drop edge at an angle θ from the vertical. The first 7 to 10 cosine coefficients are sufficient to define the series. The coefficients c_n for $n = 0$ to 9 were derived theoretically by Pruppacher and Pitter (1971) and are dependent upon drop size. The area of contact, $A(t)$, is then

$$A(t) = \pi(a^2 - (a_0 - vt)^2) \quad [4]$$

where t is the time from initial drop to solid contact and a_0 is the radius at $\theta = 0$ and $t = 0$. Thus the force during impact would be

$$F(t) = \rho v^2 A(t) \quad [5]$$

where $A(t)$ is given in Eq. [4] and ρ is the fluid density. The theoretical force vs. time curve, as described by Eq. [5], of a non-viscous, incompressible "water" drop with a diameter of 5 mm and a velocity of 9 m/s is given in Fig. 1.

In reality, the water drop impacting a solid surface behaves as a compressible fluid. On impact a compressional wave is propagated through the drop from the contact points. Hence, for a short time during impact, the fluid behaves as a compressible (elastic) material and the impact must be described using compressible mechanics. Kinner (1967) states that the duration of compressible behavior is approximated by $2vr/C^2$, where C is the velocity of sound in water (about 1500 m/s for water at 20°C). For a 5-mm diam drop with an impact velocity of 9 m/s, the duration of the compressible phase would be of the order of 0.02 μ s. The area of impact, $A(t)$, at that time would be, using Eq. [3] and [4], about 2300 μ m².

The maximum instantaneous contact pressure during the compressible phase of impact may be approximated by the "water hammer" pressure (Adler, 1979), P_w , where

$$P_w = \rho Cv. \quad [6]$$

Note that P_w is independent of drop size per se and varies only with impact velocity for a given fluid density and velocity of sound (although drop velocity is a function of size for a given height of fall). During impact, the pressure distribution on the contact area is not uniform but exhibits an annular-shaped stress concentration on the drop perimeter (Ghadiri and Payne, 1981; Huang et al., 1982; Engel, 1955). Engel (1967) predicted that the average pressure, P_{avg} , over the area of contact at the time of peak pressure, is proportional to the water hammer pressure and is given as

$$P_{avg} = \alpha / 2 (\rho Cv) \quad [7]$$

where α is a theoretically derived coefficient which is a function of the geometry of the system. α is about 0.4 for a waterdrop impacting a solid planer surface (Engel, 1967). For the 5-mm diam drop with a velocity of 9 m/s, P_{avg} is about 2.7 MPa. The maximum $A(t)$ during the compressible phase was calculated previously for this drop. The maximum force which could occur at this time is equal to P_{avg} times $A(t)$ which for this drop is about 6.2 mN. As will be shown from the results of this study, forces of drop impact are much higher than this and occur after the previously calculated duration of the compressible phase of impact.

Ghadiri and Payne (1981) measured maximum impact stresses of waterdrops by penetration of the drops through nylon meshes, from analysis of splash rebound measurements from high speed photography, and from the output of a miniature force transducer. They used two drop sizes, 6.2 and 3.5 mm diam, with height of fall ranging from 0.7

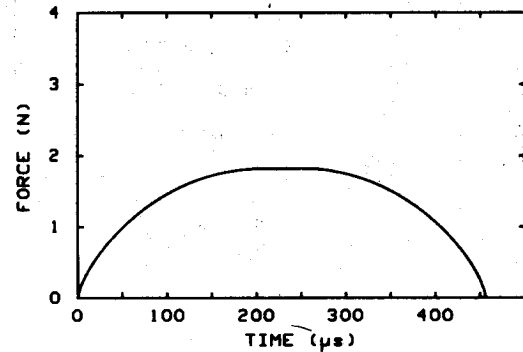


Fig. 1. Theoretical force vs. time curve for inviscid incompressible waterdrop with a diameter of 5 mm and impact velocity of 9 m/s.

to 6.2 m. Maximum stresses of about 2 to 6 MPa were found for a duration of about 50 μ s on the perimeter of a circle around the drop center. The values of stress obtained by Ghadiri and Payne were of the order of those computed from Engel's (1967) formula (i.e., Eq. [7]).

Huang et al. (1982) used a finite difference technique to solve the Navier-Stokes equations for inviscid, incompressible flow for the waterdrop impact problem. Fluid velocity distributions and the pressure distributions within the drop and at the fluid-solid contact during an impact were calculated. The assumption of incompressible behavior was an approximation, as was previously discussed. They considered that the compressible phase is so short compared to the incompressible phase, on the order of nanoseconds as compared to microseconds, that it may justifiably be neglected. The possible effect of drop surface tension was also neglected. Huang et al. (1983) used the loading conditions obtained from the previous study to compute the elastic deformations of the solid surface under impact. Results of the impact deformations were related to the soil splash mechanism.

MATERIALS AND METHODS

The force vs. time curves of waterdrop impact were measured using piezoelectric transducers. The high frequency response, fast rise time, and high sensitivity of piezoelectric transducers made them a logical choice for measuring transient waterdrop impact forces. Two transducers were used: a Kistler³ model 607C1 pressure transducer (hereafter referred to as transducer A) and a PCB model 113A02 pressure transducer (hereafter referred to as transducer B). Both were calibrated for force. Transducer A had a sensing area of 6.45 mm in diameter and transducer B had a sensing area of 5.54 mm in diameter. Although force versions of the transducers were available which were equivalent in every way to the pressure versions except for the external casings, the pressure transducers were chosen because their casings were sealed to prevent fluid from entering and shorting or corroding the internal electronics.

The signal from the transducers was amplified by a Kistler³ model 5004 charge amplifier. Interchangeable plug-in filters were used on the amplifier to dampen parasitic high frequency noise from the input signal. The choice of filter frequency was based on the resonant frequency of the transducer and was a compromise between decrease in signal rise time and increase in signal smoothness. Kistler (1984) suggests that the optimum ratio of filter frequency, f_f , to transducer frequency, f_t , is about 0.33. We found this ratio to be

³ Trade names and company names, included for the benefit of the reader, do not imply endorsement or preferential treatment of the product listed by the USDA.

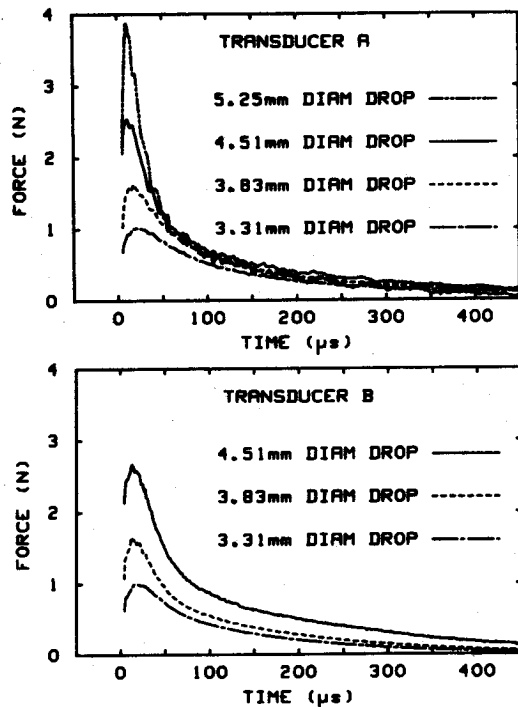


Fig. 2. Measured force vs. time curves: a. from transducer A b. from transducer B.

nearly optimal for our experimental conditions. A filter of 68 000-Hz frequency was chosen for transducer A, which had a resonant frequency of 250 000 Hz. The ratio of f_d/f_r was therefore 0.27. The rise time of the system was $0.35/f_r$ (Kistler, 1984) which in this case was $5.1 \mu\text{s}$. A 180 000-Hz filter was used with the transducer B, which had a resonant frequency of 450 000 Hz. The ratio f_d/f_r was therefore 0.40 and the rise time was $1.9 \mu\text{s}$.

The transducers were calibrated in a shock tube (Bowersox, 1958; Schweppe et al., 1963). The shock tube provides pressure steps with rise times on the order of $1 \mu\text{s}$ (Bowersox, 1958). Transducer A had a highly linear response to applied force over the range of forces encountered in this experiment. The rise time response to the pressure steps was between 5 and $6 \mu\text{s}$. We were not able to calibrate transducer B in the shock tube due to technical problems with the transducer which occurred after the measurements of drop impact force were made. Therefore, we used the manufacturer's calibration constant for that transducer. As will be seen from the data, however, the magnitude of measured force was the same for both transducers. We assumed, therefore, that the manufacturer's calibration for that transducer was correct for the dynamic impact measurements.

Force vs. time curves were measured on 3.31-, 3.83-, 4.51-, and 5.25-mm diam drops. The mean and variation of the drop sizes were determined by weighing 10 drops to the nearest 0.1 mg. The 5.25-mm drops were not measured with transducer B due to its smaller size of sensing area. The raindrop tower designed by Al-Durrah and Bradford (1981) was used to produce the drops. The height of fall for the drops was 14.0 m. The corresponding velocities for those drops at 14.0-m fall height were obtained from the data of Laws (1941). Velocity increases with drop size and was 8.32, 8.75, 9.07, and 9.29 m/s respectively for the four drop sizes used, which was essentially terminal velocity for those drops (Gunn and Kinzer, 1949). The characteristics of the drops are given in Table 1.

Many of the drops which impacted the transducer did not fall wholly on the sensing surface. The drops which fell partially on the edge of the sensing area could be determined

Table 1. Waterdrop characteristics.

Drop diameter		Drop mass		Velocity
\bar{x}	s	\bar{x}	s	
mm		mg		m/s
3.31	0.01	19.0	0.2	8.32
3.83	0.02	29.4	0.4	8.75
4.51	0.02	48.0	0.7	9.07
5.25	0.03	75.6	1.1	9.29

Table 2. Measured peak forces and time of impact to peak forces.

Transducer	Drop diameter	Peak force		Time to peak		Number of observations n
		\bar{x}	s	\bar{x}	s	
	mm	N		μs		
A	3.31	1.03	0.14	21.2	1.2	15
	3.83	1.65	0.27	19.3	2.9	15
	4.51	2.55	0.29	15.4	2.9	15
	5.25	3.76	0.21	13.9	4.0	8
B	3.31	0.97	0.08	14.4	1.4	15
	3.83	1.61	0.05	13.9	1.5	11
	4.51	2.59	0.30	13.1	1.4	15

from the splash pattern on the Al block on which the transducers were mounted. Those drops which fell completely on the sensing area formed a single ring centered around the transducer after impact. Erroneous data due to drop impingement on the sensor edge was eliminated in this way during data collection.

The force input signal was recorded on a Hewlett-Packard model 5182A waveform recorder at a rate of one point per microsecond for a period of $512 \mu\text{s}$ for each impact. Between 8 and 15 impacts were recorded for each drop size on each transducer. The mean and variation of both maximum impact force and time to maximum impact force were determined for each drop size and transducer data set. Representative curves which approximated mean force and time to peak values were selected from the data sets. Average pressure vs. time was determined from the force divided by the contact area as calculated from Eq. [4].

RESULTS AND DISCUSSION

Waterdrop Forces

The representative force vs. time curves measured by the two transducers are shown in Fig. 2. The curves were assumed to be valid for t greater than the transducer rise times, hence, the curves begin at $t = 6 \mu\text{s}$ for transducer A and at $t = 3 \mu\text{s}$ for transducer B. The peak impact forces occurred within the valid time range of measurement and hence may be considered to be accurate. Table 2 lists the peak forces and times to peak for each of the drop sizes and each transducer. The forces decayed to 0.5 N after approximately $100 \mu\text{s}$. As expected, peak force increased with drop size. No attempt was made in this study to correlate peak waterdrop impact forces to drop properties.

The measured time to peak force ranged from 13 to $21 \mu\text{s}$ and tended to decrease with increasing drop size, but was not the same for both transducers. Transducer A measured a longer time to peak than did transducer B in each case. This is probably due to the slower rise time of transducer A.

The force vs. time curves of impact are very different from that calculated using Eq. [4] for an incompressible drop as shown in Fig. 1. Both the theoretical

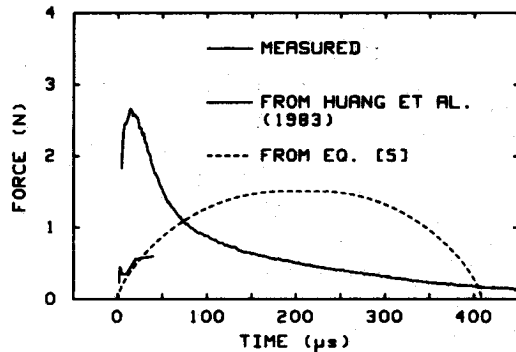


Fig. 3. Force vs. time curves for the 4.51-mm diam drop as measured with transducer B, as calculated from Eq. [5], and as integrated from the numerically derived data of Huang et al. (1983).

(based on Eq. [4]) and measured force vs. time curves for the 4.51-mm drop are plotted in Fig. 3. The difference suggests that by ignoring the compressible behavior of the drop during impact, an important aspect in understanding the process of impact is lost.

The pressure distribution data of Huang et al. (1983, Fig. 2) was integrated over the area to obtain total force. The data for the 4.51-mm diam drop was plotted in Fig. 3 for force. The numerical technique underestimates the forces of drop impact. A possible reason for this is that the compressible behavior of the drop, which was ignored in the numerical solution on the basis of its assumed short duration, may in fact have a longer lasting effect than was assumed by Huang et al. The difference between measured and computed impact forces could also be due to water surface tension or viscous effects, which were ignored in the numerical solution. A numerical experiment would need to be performed to delineate between the possible effects of water compressibility and surface tension or viscosity on waterdrop impact forces.

Calculated Pressures

The curves in Fig. 4 of average pressure vs. time, calculated from the force data and with Eq. [4] for $A(t)$, indicated that the pressure peaks occurred before the 3 or 6 μs limitations of the transducers and hence were not recorded. The pressure curves were, however, accurate starting at 6 μs for transducer A and at 3 μs for transducer B. According to Engel's theory, peak pressure should be dependent only on drop velocity and not drop size. However, the pressure after peak will decrease faster the smaller the drop size. This was consistent with the observed results. The results, therefore, do not necessarily suggest that larger drops exhibit greater peak impact pressures, but they do indicate that the high pressures occur for a greater duration and hence over a greater area for the larger drops. From the measurements of transducer B, for example, average pressure of greater than 500 kPa were present for about 7 μs in the case of the 3.31-mm diam drop and for about 17 μs in the case of the 4.51-mm diam drop. By 50 μs the pressure for all the drop sizes is reduced to approximately 100 kPa.

The maximum average pressure calculated from the force measurements was for the 5.25-mm diam drop and was 1.3 MPa. This must be considered to be, based on the fact that the actual peak pressures could not be

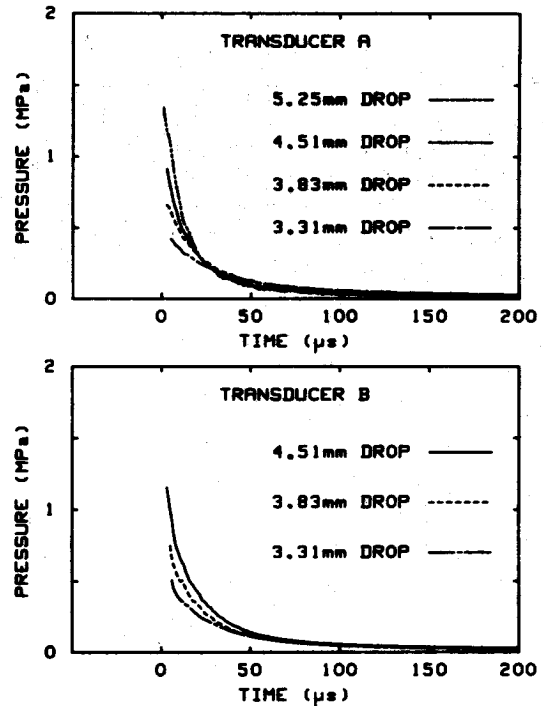


Fig. 4. Average pressure vs. time as calculated from the measured force and Eq. [4]: a. from transducer A b. from transducer B.

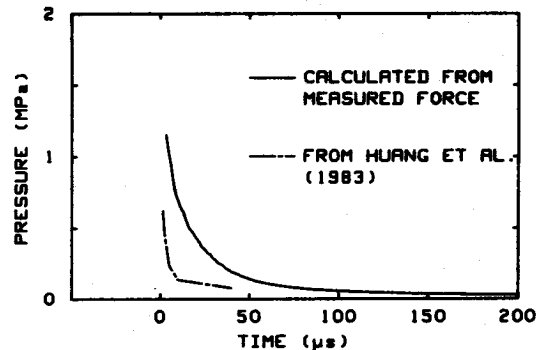


Fig. 5. Average pressure vs. time for the 4.51-mm diam drop as calculated from the force measured with transducer B and Eq. [4], and as obtained from the data of Huang et al. (1983).

recorded, a conservative measurement, and in fact was about half of Engel's predicted value (using Eq. [7]) of peak average pressure which is 2.7 MPa.

The average pressure from the calculations of Huang et al. (1983) was plotted in Fig. 5 along with the calculated pressures from the measured force data. The numerical technique underestimates the pressures of drop impact. Again, the difference may be due to compressibility, surface tension, and/or viscous effects which were not considered in the numerical model.

Implications

The measurements of impact forces and the pressures calculated from those forces indicate that theory or numerical techniques that do not take into account compressional wave generation, surface tension, or viscosity, do not predict the actual behavior well. The theory which describes the compressible behavior, such as Engel's, suggests very high pressures for a very short duration after the initial contact, which agrees quali-

tatively with the measured data. The possible effects of surface tension or viscosity are not known. Surface tension and viscosity may have a similar effect on the force vs. time relationships or their effects may be negligible. Further research is needed to delineate the effects of compressibility, surface tension, and viscosity on waterdrop impact forces; however, it is apparent that by ignoring their effects the impact phenomenon is not well described.

CONCLUSIONS

The results of this study may be summarized as follows:

1. Peak force ranged between 1.0 and 3.8 N for the 3.31, 3.83, 4.51, and 5.25-mm diam drops tested, occurred within about 13 to 21 μ s after initial contact, and decreased to 0.5 N after approximately 100 μ s. These curves are very different from those that would be expected by assuming the drop during impact to be incompressible and have no surface tension or viscosity.
2. The average pressure curves increased and decreased much more quickly than did the force curves because of the increase of contact area with impact time. Peak impact pressures occurred before 3 μ s and could not be measured with the equipment used. The results showed that high impact pressures occurred over a longer time period for the larger drops. Average pressures of over 500 kPa were present for about 7 μ s in the case of the 3.31-mm diam drop, and for about 17 μ s for the 4.51-mm diam drop as measured with transducer B.
3. The data from this investigation suggests that the times and magnitudes of forces and average pressures of impact are not well predicted from theory using incompressible mechanics nor by the numerical technique applied by Huang et al. (1982), which assumes incompressible fluid behavior and ignores surface tension effects and viscosity.

ACKNOWLEDGMENT

The authors want to thank Dr. J. Katz for his advice concerning the dynamic calibration of the transducers, and B. Nattermann and J. Williams for their technical assistance.

REFERENCES

- Adler, W.F. 1979. The mechanics of liquid impact. p. 127-183. *In* C.M. Preece (ed.) *Treatise on material science and technology*, Vol. 16. Academic Press, New York.
- Al-Durrah, M.M., and J.M. Bradford. 1981. New methods of studying soil detachment due to waterdrop impact. *Soil Sci. Soc. Am. J.* 45:949-953.
- Al-Durrah, M.M., and J.M. Bradford. 1982a. Parameters for describing detachment due to single waterdrop impact. *Soil Sci. Soc. Am. J.* 46:836-840.
- Al-Durrah, M.M., and J.M. Bradford. 1982b. The mechanism of raindrop splash on soil surfaces. *Soil Sci. Soc. Am. J.* 46:1086-1090.
- Bowersox, R. 1958. Calibration of high-frequency-response pressure transducers. *Instrument Soc. Am. J.* 5:98-103.
- Cruse, R.M., and W.E. Larson. 1977. Effect of soil shear strength on soil detachment due to raindrop impact. *Soil Sci. Soc. Am. J.* 41:777-781.
- Engel, O.G. 1955. Waterdrop collisions with solid surfaces. *J. Res. Nat. Bur. Stand.* 54:281-298.
- Engel, O.G. 1967. Discussion of paper by F.J. Heymann. p. 741-747. *In* A.A. Fyall and R.B. King (ed.) *Proc. of the second Meersburg conf. on rain erosion and allied phenomena*, Vol. 2. Royal Aircraft Establishment, Farnborough, England.
- Ghadiri, H., and D. Payne. 1977. Raindrop impact stress and the breakdown of soil crumbs. *J. Soil Sci.* 28:247-258.
- Ghadiri, H., and D. Payne. 1981. Raindrop impact stress. *J. Soil Sci.* 32:41-49.
- Gunn, R. and G.D. Kinzer. 1949. The terminal velocity of fall for water droplets in stagnant air. *J. Meteorology.* 6:243-248.
- Huang, C., J.M. Bradford, and J.H. Cushman. 1982. A numerical study of raindrop impact phenomena: The rigid case. *Soil Sci. Soc. Am. J.* 46:14-19.
- Huang, C., J.M. Bradford, and J.H. Cushman. 1983. A numerical study of raindrop impact phenomena: the elastic deformation case. *Soil Sci. Soc. Am. J.* 47:855-861.
- Imeson, A.C., R. Vis, and E. de Water. 1981. The measurement of waterdrop impact forces with a piezoelectric transducer. *Catena* 8:83-96.
- Kinner, G.H. 1967. Some remarks on single impact studies at the Royal Aircraft Establishment. p. 517-529. *In* A.A. Fyall and R.B. King (ed.) *Proc. of the second Meersburg conf. on rain erosion and allied phenomena*, Vol. 2. Royal Aircraft Establishment, Farnborough, England.
- Kistler Staff. 1984. Low-pass plug-in filters. Kistler Instruments, Amherst, N.Y.
- Laws, J.H. 1941. Measurements of the fall-velocity of water drops and raindrops. *Trans. Am. Geophys. Union* 22:709-721.
- Nearing, M.A. and J.M. Bradford. 1985. Single waterdrop impact detachment and mechanical properties of soils. *Soil Sci. Soc. Am. J.* 49:547-552.
- Palmer, R.S. 1965. Waterdrop impact forces. *Trans. ASAE* 8:69-72.
- Pruppacher, H.R. and R.L. Pitter. 1971. A semi-empirical determination of the shape of cloud and rain drops. *J. Atmos. Sci.* 28:86-94.
- Schweppe, J.L., L.C. Eichberger, D.F. Muster, E.L. Michaels, and G.F. Paskusz. 1963. Methods for the dynamic calibration of pressure transducers. *Natl. Bureau of Standards Monogr.* 67. U.S. Gov. Printing Office, Washington DC.